Nuclear Instruments and Methods in Physics Research A 648 (2011) 109–113

Contents lists available at ScienceDirect

Nuclear Instruments and Methods in Physics Research A

journal homepage: www.elsevier.com/locate/nima

Channel selection of neutron-rich nuclei following fusion-evaporation reactions of light systems

J. Gibelin [a,*], M. Wiedeking [a,b,c], L. Phair [a], P. Fallon [a], S. Basunia [a], L.A. Bernstein [b], J.T. Burke [b], D.L. Bleuel [a,b], R.M. Clark [a], M. Cromaz [a], M.-A. Deleplanque [a], B.F. Goldblum [b,d,1], S. Gros [a], H.B. Jeppesen [a], P.T. Lake [a,d], I.-Y. Lee [a], S.R. Lesher [b], A.O. Macchiavelli [a], M.A. McMahan [a], J. Pavan [a], E. Rodriguez-Vieitez [a,d], N.D. Scielzo [b], L.G. Moretto [a,d]

[a] Lawrence Berkeley National Laboratory, Berkeley, CA 94720, USA
[b] Lawrence Livermore National Laboratory, Livermore, CA 94550, USA
[c] iThemba LABS, P.O. Box 722, 7129 Somerset West, South Africa
[d] University of California, Berkeley, CA 94720, USA

ARTICLE INFO

Article history:
Received 7 March 2011
Received in revised form
30 April 2011
Accepted 16 May 2011
Available online 2 June 2011

Keywords:
Fusion-evaporation reactions
Light nuclei
γ-Spectroscopy

ABSTRACT

Experimental results for the minor decay channels of fusion-evaporation in light projectile plus light target systems are presented. These new data were obtained during test campaigns to measure the opening of different decay channels. Experiments were designed to provide relative cross-section information on weakly populated channels for gamma-ray spectroscopy experiments in coincidence with charged-particles. The results are compared to publicly available fusion-evaporation codes. The data follow a simple estimate which is useful in predicting experimental conditions to make the fusion-evaporation reaction a viable nuclear structure tool to study weakly populated light neutron-rich nuclei.

1. Introduction

The fusion-evaporation reaction, in conjunction with γ-spectroscopy, is widely used as a tool to study nuclear structure. Fusion reactions have been studied extensively in medium mass and heavy nuclei, but only marginally in (very) light nuclei to evaluate minor decay channels of rather exotic species. Recent experiments performed at the Lawrence Berkeley National Laboratory 88-in. Cyclotron provided a clean extraction of the two-proton evaporation channel [1,2] and called for understanding the reaction mechanisms in order to predict the opening and closing of different decay channels.

Most of the available fusion-evaporation codes predict comparable results for the dominant decay channels but the calculated results for weaker channels are found to be discrepant. Here, results from different experiments designed to identify some of the major and minor decay channels of interest are gathered and compared with various theoretical calculations.

2. Experimental procedures

The results presented in this article have been obtained from several experiments carried out at the 88-in. Cyclotron at Lawrence Berkeley National Laboratory. In these experiments, the emitted γ-radiation and charged-particles were detected with the STARS-LIBERACE detector array [3], which consists of large area segmented annular silicon detectors (arranged in a ΔE–E telescope) and up to six Compton suppressed HPGe Clover detectors [4,5].

The first experiment studied the ^{9}Be+^{9}Be system at beam energies of 30, 35, and 40 MeV. The average beam current was approximately 0.1 pnA over a period of 3 days and the ^{9}Be target had a thicknesses of 2.6(1) mg/cm^2. Five Clover detectors were placed at 16.5(5) cm from the target. Two Clovers were located at 40°, one at 90° and two at 140°, relative to the beam direction. The charged-particle telescope comprised two Micron Semiconductor S2-type silicon detectors [6] (22 mm active inner diameter and 70 mm active outer diameter): a 152 μm as ΔE detector and a 1003 μm as E detector. The ΔE detector was mounted 30(2) mm downstream from the target. The ΔE–E separation was 3(1) mm, hence an acceptance for charged-particles of about 35° to 65°. A thick 56.7 mg/cm^2 lead foil spanned the front of the ΔE detector to suppress α particles from the break-up of ^{9}Be as well as screen δ-electrons coming from the target.

* Corresponding author. Present address: LPC-Caen/Université de Caen, 14050 Caen cedex, France.
E-mail address: gibelin@lpccaen.in2p3.fr (J. Gibelin).
[1] Present address: University of Tennessee, Knoxville, TN 37996, USA.

0168-9002/$ - see front matter © 2011 Elsevier B.V. All rights reserved.
doi:10.1016/j.nima.2011.05.041

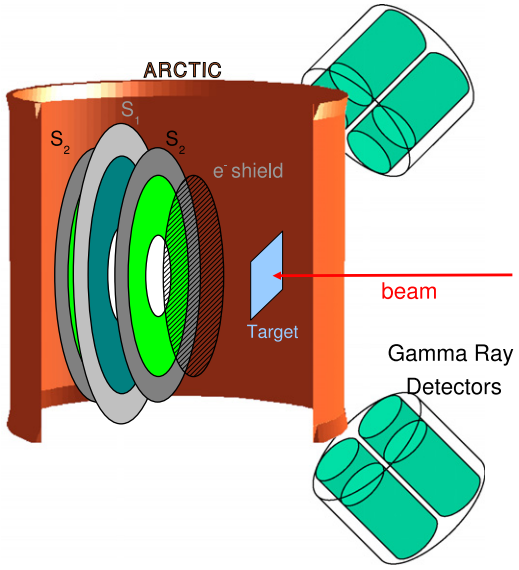

Fig. 1. Schematic of the second experimental setup. The telescope comprised three silicon detectors (S2-S1-S2) with the electron shield and target in front. These detector are confined within the copper-radiator ARCTIC cooled at 0 °C. The figure also shows two of the five germanium detectors.

The second experiment was the $^{18}O+^{11}B$ reaction at 50 and 60 MeV bombarding energies. The average beam current was approximately 0.1 pnA over a period of 2.5 days. The ^{11}B target was generated from 99.65% ^{11}B powder baked onto a 100 $\mu g/cm^2$ foil of ^{12}C using the techniques described in Ref. [7]. The total thickness was measured by α energy loss to be approximately 450 $\mu g/cm^2$ (*i.e.* a maximum of 310 $\mu g/cm^2$ of Boron). For this experiment, one Clover detector was moved from 40° to 90°, so only one remains at 40°. In order to increase the solid angle covered by the telescope, an additional *E* detector, 1001 μm Micron S1-type silicon detectors (active area between diameters of 48 and 96 mm) were inserted 10(1) mm beyond the ΔE and 3(1) mm in front of the last *E* detector, see schematics in Fig. 1. This leads to an acceptance between 40° and 75° in laboratory frame. This telescope was located approximately 15 mm downstream from the target and was protected by 250 $\mu g/cm^2$ of aluminized Mylar, biased to help shield the detectors from electrons coming from the target. Finally, in order to improve the silicon energy resolution, a radiative cooling system—named ARCTIC [8][2]—was placed inside the reaction chamber and maintained the silicon detectors at ~15 °C. This apparatus consists of a cylindrical sheet of copper cooled by a closed circuit of ethylene glycol to a temperature just above 0 °C. The setup was insulated from the reaction chamber by an additional, thermally isolated, aluminum layer.

In both experiments, the on-line trigger required the detection of at least one charged-particle. Coincident γ-ray events were recorded to disk if they were accompanied by a particle trigger. In the offline analysis, the particle–particle coincidence time interval was reduced to the order of the corresponding cyclotron radio frequency period (< 100 ns), and a time spectrum between the γ-ray and the particle trigger was used to reject uncorrelated γ-particle events. Germanium detector energie dynamic range was set up to 8 MeV and calibrations were performed using standard ^{56}Co, ^{152}Eu and ^{228}Th γ-ray sources. The ^{152}Eu source was also used for a relative efficiency measurement as well as an absolute measurement [9]. The silicon detectors were calibrated using α emitted from a ^{226}Ra source. For more details about the experimental setup and techniques the reader is referred to Ref. [3]. In all experiments sufficient data were collected in 12–24 h to perform a spectroscopic analysis.

[2] A Radiative Cooling Thermostat Inside Chamber.

3. Analysis

The levels of each nucleus of interest were studied and the excited state closest to the ground state that decays by γ emission used as a signature of its production. The nuclei studied are light and thus their level schemes are sparse enough to characterize them this way. Different decay paths were selected by applying gates on the different outgoing charged-particles emitted in coincidence with the emission of a γ-ray. This is equivalent to select the production of certain rare isotopes that can lead to their possible γ-spectroscopy.

For the experiments performed with the ^{18}O beam, the ^{11}B target was deposited on a ^{12}C foil; therefore, the reaction products from the carbon backing are also measured. Ambiguities on the identification of the different species are generally resolved on the basis of *Q*-value and excitation energy arguments. In those cases where the γ intensity was strong enough, a $\gamma-\gamma$ analysis was performed to confirm our first deductions.

Fig. 2 presents the γ energy distribution obtained in the ^{18}O (50 MeV)$+^{11}B$ reaction for three different gates: 1p, 1α and 2p. The products of the reactions on the carbon backing are also clearly visible. This figure also illustrates the clean nucleus identification based on particle(s)/γ coincidence: for example, the 94 keV gamma lines of ^{24}Na coming essentially from the $^{11}B(^{18}O, \alpha n)^{24}Na$ reaction are clearly seen in the alpha gates but absent in the one proton and two proton gates. The same is also true for the ^{28}Mg, generated by reaction on the ^{12}C and formed by the evaporation of two protons, which can only be seen in the two proton gate.

Results from the $^{9}Be+^{9}Be$ reaction are similar both in their cleanliness and in the number of lines observed (on average: one or two per nucleus).

4. Results and discussion

In this section the experimental results are compared to fusion-evaporation codes of simple predictions, in order to

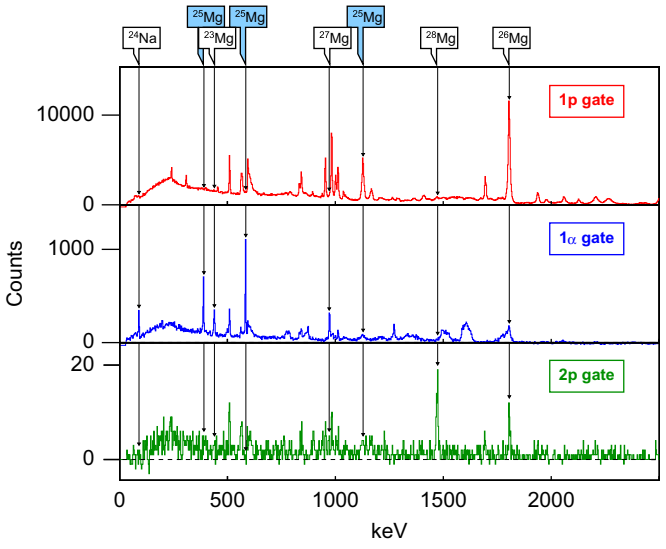

Fig. 2. Example of clean decay channel selection. The gamma energy distribution at 90° (no-Doppler) obtained with the ^{18}O + ^{11}B reaction at 50 MeV is gated with the detection of one proton (top), one alpha (middle) and two protons (bottom). The nuclei identified are specified at the top of the figure (see text for details).

determine how helpful they are in predicting the opening of decay channels of interested. Four different programs were used: PACE4 [10,11], LisFus [11] (both included with LISE++ version 9.1.23 [18]) GEMINI [12] and a simple Hauser-Feshbach calculation (HF) [13]. Note that when available, the calculated cross-section deduced with GEMINI and HF is obtained by folding the decay probability with the experimental fusion cross-section σ_f [14] (instead of the Bass model) with improved results.

As a first test, these codes' outputs are compared with data from the previously measured ^{11}B(^{18}O, pn)^{27}Mg reaction [15], using also gamma-ray emission for identification. The results are presented in Fig. 3 where the theoretical and experimental yields—corrected from gamma efficiency—agree reasonably well as a function of bombarding energy. The predicted cross-section however drops slowly at high energy compared with the experimental data [15]. The data presented here—as explained in the following—could not be absolutely normalized but are compatible with the slow decrease in the calculations (see Fig. 3).

These experiments were not designed with the intent of extracting absolute cross-sections and if the results do include the gamma-ray efficiency the charged-particles one is not included. In order to avoid ambiguities in comparing the different yields this was only accomplished when the different species were produced within the same particle gate. We assume that the detection efficiency for one gate is comparable for all nuclei produced and their differences are negligible compare to other errors. Three clean particle gates are analyzed: one proton, two protons and one alpha in coincidence with gamma-transition. The corresponding nuclei considered here and the observed γ-rays are summarized in Table 1. The ^{11}B target had a ^{12}C backing so γ-lines can come from reactions on either ^{11}B or ^{12}C. When there are no ambiguities only one "target" is specified in Table 1.

Tables 2–4 present experimental yield ratios of the observed nuclei. The first two tables are relative yield ratios within the same particle gate and the third table is a relative excitation function, normalized to the yield obtained with the highest incident energy. Note that the beam energy is calculated at the center of the target.

Since these experiments were designed to observe the two-proton emission channel, the discussion is focused on this decay channel.

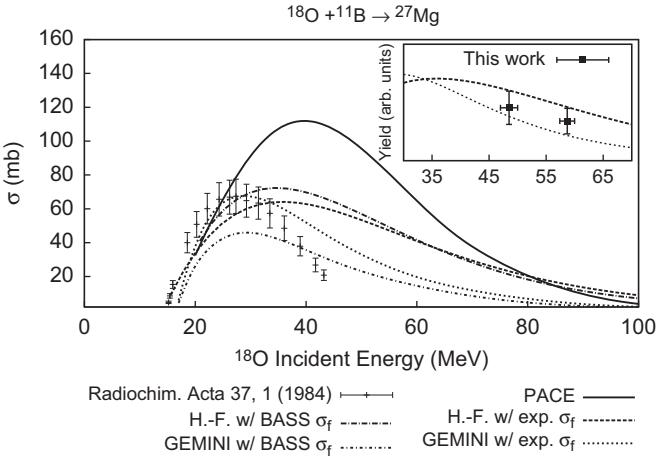

Fig. 3. ^{11}B(^{18}O, pn)^{27}Mg reaction cross-section obtained experimentally by M. Rousseau et al. [15] (points with error bars) is compared with HF, GEMINI and PACE calculations as a function of incident energy. For GEMINI and HF the calculation is performed without and with experimental fusion cross-section (see text for details). These last results are compared to our work in the insert, where data and calculations are arbitrary normalized: the relative yields between the calculations and between our data were kept, only the scale between theory and experiment is arbitrary.

Table 1
Observed γ-ray lines and consequent nucleus identification for the indicated reactions using different charged-particle gates.

Projectile	Target	Gate→Nucleus	E_γ KeV
^{18}O + ^{11}B/^{12}C		1p→^{26}Mg	1808
		1p→^{27}Mg	985
		1α→^{24}Na	91
		1α→^{25}Mg	585
^{18}O + ^{12}C		2p→^{27}Mg	985
		2p→^{28}Mg	1470
^{9}Be + ^{9}Be		1p→^{15}N	1884
			5264
		1p→^{16}N	297
		1α→^{12}C	4400
		1α→^{13}C	168
		2p→^{15}C	741
		2p→^{16}C	1758

Table 2
Summary table of production yield ratios for the ^{9}Be+^{9}Be reactions. The beam energy and its errors account for the energy loss in the target and the error on the exact reaction point. Note that, following Table 1, ^{15}N production yield has been obtained from different γ yields (1884 and 5264 keV).

Gate	Nuclei (E_γ gate)		Production yield ratio at beam energy (MeV)		
			28.0 ± 2.0	33.2 ± 1.8	38.4 ± 1.6
1p	over	^{15}N (1.9 MeV) ^{16}N	0.7 ± 0.2	1.8 ± 0.4	5.1 ± 1.1
	over	^{15}N (5.3 MeV) ^{16}N	2.4 ± 0.5	3.1 ± 0.7	6.0 ± 1.3
1α	over	^{12}C ^{13}C	6.8 ± 1.4	12.0 ± 2.6	32.2 ± 6.9
2p	over	^{15}C ^{16}C	0.04 ± 0.06	0.09 ± 0.04	0.36 ± 0.11

Table 3
Summary table of production yield ratios for the ^{18}O+^{11}B and ^{18}O+^{12}C reactions described in this article. The origin of errors is identical as for the ^{9}Be+^{9}Be reaction in Table 2.

Gate	Nuclei (Target)		Production yield ratio at beam energy (MeV)		
			48.5 ± 1.5	53.6 ± 1.4	58.7 ± 1.3
1p	over	^{26}Mg (^{11}B) ^{27}Mg (^{11}B)	2.6 ± 0.53	3.7 ± 0.82	4.8 ± 0.91
1α	over	^{24}Na (^{11}B) ^{25}Mg (^{12}C)	0.55 ± 0.38	0.48 ± 0.33	0.76 ± 0.52
2p	over	^{27}Mg (^{12}C) ^{28}Mg (^{12}C)	0.23 ± 0.08		0.89 ± 0.25

The excitation function of ^{15}C from the ^{9}Be+^{9}Be reaction, presented in Table 4, is an example of practical application of the data. The ^{15}C relative production yield at 30 MeV incident energy is compatible with zero and slowly rises with the incident energy. This can be interpreted as the opening of the ^{15}C channel *via* the emission of one neutron and two protons and that leads to a 741 keV gamma-ray from the first excited state of the nucleus.

In an attempt to predict the best incident energy that provides sufficient energy to perform gamma-ray spectroscopy of light neutron-rich nuclei, the ratios of the γ-ray yields (corrected for energy dependent γ-ray detection efficiency) are compared with

Table 4
Summary table of relative production yield ratios for all the reaction presented in this article. These excitation functions are normalized to the highest incident energy. For ^{15}N (a) and (b) are the yield obtained with the identification of a γ-ray of 1884 keV and 5264 keV respectively.

Reaction	Production yield ratio at beam energy (MeV)	
	48.5 ± 1.5	58.7 ± 1.3
^{11}B(^{18}O, p2n)^{26}Mg	0.71 ± 0.21	**1**
^{11}B(^{18}O, pn)^{27}Mg	1.32 ± 0.40	**1**
^{11}B(^{18}O, αn)^{24}Na	0.55 ± 0.17	**1**
^{12}C(^{18}O, αn)^{25}Mg	0.76 ± 0.23	**1**
^{12}C(^{18}O, n2p)^{27}Mg	0.24 ± 0.01	**1**
^{12}C(^{18}O, 2p)^{28}Mg	0.93 ± 0.02	**1**

Reaction	Production yield ratio at beam energy (MeV)		
	28.0 ± 2.0	33.2 ± 1.8	38.4 ± 1.6
^{9}Be(^{9}Be, p2n)^{15}N (a)	0.32 ± 0.10	0.31 ± 0.09	**1**
^{9}Be(^{9}Be, p2n)^{15}N (b)	0.89 ± 0.27	0.45 ± 0.14	**1**
^{9}Be(^{9}Be, pn)^{16}N	2.25 ± 0.68	0.88 ± 0.26	**1**
^{9}Be(^{9}Be, α2n)^{12}C	0.27 ± 0.08	0.29 ± 0.09	**1**
^{9}Be(^{9}Be, αn)^{13}C	1.28 ± 0.38	0.78 ± 0.24	**1**
^{9}Be(^{9}Be, n2p)^{15}C	0.02 ± 0.03	0.10 ± 0.03	**1**
^{9}Be(^{9}Be, 2p)^{16}C	0.16 ± 0.06	0.36 ± 0.09	**1**

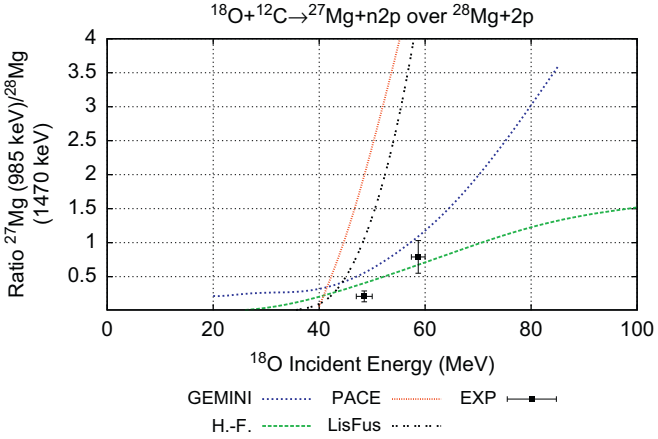

Fig. 4. The production yield ratio between ^{27}Mg and ^{28}Mg obtained in the ^{18}O+^{12}C reaction in coincidence with the identification of two protons is plotted as a function of the projectile incident energy. Points are experiment, the dotted and dashed lines are results from GEMINI calculation (blue), H.-F. (green), PACE (red) and LisFus (black). (For interpretation of the references to color in this figure legend, the reader is referred to the web version of this article.)

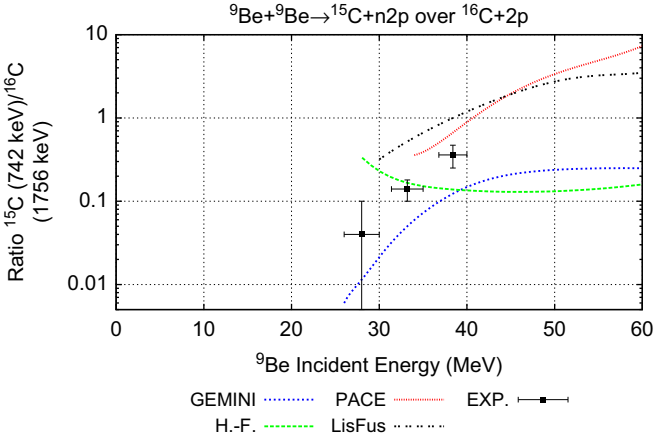

Fig. 5. Production yield ratio between ^{15}C and ^{16}C obtained in the ^{9}Be+^{9}Be reaction in coincidence with the identification of two protons, function of the projectile incident energy. Legend identical to Fig. 4.

PACE4, LisFus, GEMINI and HF results for the two proton gate for the ^{18}O+^{12}C reaction in Fig. 4, and the ^{9}Be+^{9}Be reaction in Fig. 5.

The ^{27}Mg and ^{28}Mg from ^{18}O+^{12}C ratio data points are in decent agreement with both the GEMINI and HF calculations, but both PACE4 and LisFus tend to overestimate the yield of the ^{27}Mg. In the case of the ratio of the ^{9}Be+^{9}Be experimental data, they seem to follow the trend of the PACE, LisFus and GEMINI calculations. However, both PACE and LisFus overestimate the yield of ^{15}C (about 3 times more) whereas GEMINI underestimate it (about twice less). The HF calculations show an increase in ratio at lower incident beam energies in contradiction to the experimental measurements. At higher energies the ratio seems to underestimate the data: the basic HF calculation is not good enough to reproduce the ^{9}Be+^{9}Be data.

A simple calculation for the expected incident beam energy (E_{inc}) to populate the 2p evaporation channel sufficiently for gamma-spectroscopic nuclear structure studies is now presented. This estimate is based on the experimental observation of 5 MeV kinetic energy (E_p) for each evaporated proton and the additional requirement to populate the system with enough remaining excitation energy (E_x of $\approx$5 MeV) following evaporation to allow for gamma-ray decay.

This estimate is

$$E_{inc} = \left(2 \underbrace{E_p}_{5\ \mathrm{MeV}} + \underbrace{E_x}_{5\ \mathrm{MeV}} - Q + S_{2p} \right) \frac{M_{\mathrm{projectile}} + M_{\mathrm{target}}}{M_{\mathrm{target}}} \quad (1)$$

where Q is the fusion Q-value, S_{2p} two proton separation threshold, $M_{\mathrm{projectile}}$ the mass of the projectile and M_{target} the target mass.

Using Eq. (1) a 2p-channel incident energy of $E_{inc} \sim 40$ MeV for both the ^{18}O+^{12}C and the ^{9}Be+^{9}Be reactions is obtained. This value is used in Ref. [2] with success. However, the ^{18}O+^{12}C reaction was experimentally performed at higher energies with the effect that the 2p-channel is still clearly present. The spectrum is certainly not overwhelmed by the opening of the 1n–2p-channel. This is partially due to the sparse level scheme of such light nuclei and the smooth decrease in the excitation function,

identical to what can be observed for 1p-channel in Fig. 3. This implies that for a study of excited states in ^{28}Mg–provided that its states can be energetically separated from ^{27}Mg ones—a higher incident energy is possible.

Finally, Eq. (1) also successfully estimates the necessary incident energy to produce light nuclei for γ-spectroscopy through 2p evaporation in ^{9}Be(^{11}B,2p)^{18}N [1] and ^{18}O(^{18}O,2p)^{34}Si [16], at beam energies of 50 and 25 MeV, respectively. This calculation also matches a previously published experiment [17].

5. Conclusion

The selection of minor decay channels from fusion-evaporation reactions producing rare species of light nuclei is described. In order to test our understanding the yield of the light nuclei produced is compared to different model predictions with mitigated success. The selection of minor decay channel is used as a tool to study the excited states of neutron-rich nuclei for relevant γ-ray measurements in coincidence with evaporated charge particles.

A simple formula to estimate the necessary incident beam energy to study weakly populated light neutron-rich nuclei following the two proton evaporation reaction is proposed. We conclude that the detection of evaporation particles in coincidence with gamma-transitions in light compound systems is a useful tool for selecting relatively weak channels for spectroscopic nuclear structure studies.

Acknowledgments

The authors thank the operations staff of the 88-in. Cyclotron. Support for Lawrence Berkeley National Laboratory was provided by the U.S. Department of Energy under Contract No. DE-AC02-05CH11231. Part of this work was performed under the auspices of the U.S. Department of Energy by the University of California, Lawrence Livermore National Laboratory under Contract No. DE-AC52-07NA27344.

References

[1] M. Wiedeking, et al., Phys. Rev. C 77 (2008) 054305.
[2] M. Wiedeking, et al., Phys. Rev. Lett. 100 (2008) 152501.
[3] S.R. Lesher, et al., Nucl. Instr. and Meth. A 621 (2010) 286.
[4] G. Duchêne, et al., Nucl. Instr. and Meth. A 432 (1999) 90.
[5] Z. Elekes, et al., Nucl. Instr. and Meth. A 503 (3) (2003) 580.
[6] Micron semiconductor ltd., 〈www.micronsemiconductor.co.uk〉.
[7] R.T. Santoro, H. Weaver, Rev. Scient. Instr. 36 (1965) 98.
[8] J. Gibelin, et al., AIP Conf. Proc. 1005 (2008) 77.
[9] N.D. Scielzo, et al., Phys. Rev. C 81 (2010) 034608.
[10] A. Gavron, Phys. Rev. C 21 (1980) 230.
[11] O.B. Tarasov, D. Bazin, Nucl. Instr. and Meth. B 204 (2003) 174.
[12] R.J. Charity, et al., Nucl. Phys. A 483 (1988) 371.
[13] G.R. Satchler, Introduction to Nuclear Reactions, second ed., Oxford University Press, 1990.
[14] R.M. Anjos, et al., Phys. Rev. C 49 (1994) 2018.
[15] M. Rousseau, C. Friedli, P. Lerch, Radiochim. Acta (1984) 1.
[16] M. Wiedeking, et al., private communication.
[17] A.D. Panagiotou, et al., Z. Phys. A 302 (1981) 117.
[18] O. Tarasov, D. Bazin, Nucl. Instr. Meth. B 266 (2008) 4657.